

Reconfigurable Meta-Radiator Based on Flexible Mechanically Controlled Current Distribution in Three-dimensional Space

NAN-SHU WU^{1,2}, SU XU^{1,2,6}, XIAO-LIANG GE¹, JIAN-BIN LIU¹, HANG REN¹, KUIWEN XU³, ZUOJIA WANG⁴, FEI GAO⁴, QI-DAI CHEN¹, AND HONG-BO SUN^{1,5,7}

¹State Key Laboratory of Integrated Optoelectronics, College of Electronic Science and Engineering, Jilin University, Changchun 130012, China

²Zhejiang Provincial Key Laboratory of Advanced Microelectronic Intelligent Systems and Applications, Hangzhou 310027, China

³Engineering Research Center of Smart Microsensors and Microsystems, Ministry of Education, School of Electronics and Information, Hangzhou Dianzi University, Hangzhou 310018, China.

⁴Interdisciplinary Center for Quantum Information, State Key Laboratory of Modern Optical Instrumentation, Zhejiang University, Hangzhou 310027, China

⁵State Key Laboratory of Precision Measurement Technology and Instruments, Department of Precision Instrument, Tsinghua University, Haidian, Beijing 100084, China

⁶xusu@jlu.edu.cn

⁷hbsun@tsinghua.edu.cn

Compiled September 12, 2023

In this paper, we provide an experimental proof-of-concept of this dynamic 3D current manipulation through a 3D-printed reconfigurable meta-radiator with periodically slotted current elements. By utilizing the working frequency and the mechanical configuration comprehensively, the radiation pattern can be switched among 12 states. Inspired by maximum likelihood method in digital communications, a robustness-analysis method is proposed to evaluate the potential error ratio between ideal cases and practice. Our work provides a previously unidentified model for next-generation information distribution and terahertz-infrared wireless communications. © 2023 Optical Society of America

<http://dx.doi.org/10.1364/ao.XX.XXXXXX>

1. Introduction

2. Theory

3. Simulation

4. Experiment

5. Discussion

6. Conclusion

7. Acknowledgments

8. References

9. Appendix

10. Author Biographies

11. Supplemental Material

12. Correspondence

13. Funding

14. Contact Information

15. Additional Resources

16. Declaration of Interest

17. Copyright

18. Terms and Conditions

19. Privacy Policy

20. Disclaimer

1] Wu

2, 3] Li

8–10] Chen

13, 14]

15] Chen

15] Chen

16] Chen

17] Chen

18] Chen

19] Chen

20] Chen

21] Chen

22] Chen

23] Chen

24] Chen

25] Chen

26] Chen

27] Chen

28] Chen

29] Chen

30] Chen

31] Chen

32] Chen

33] Chen

34] Chen

35] Chen

36] Chen

37] Chen

38] Chen

39] Chen

40] Chen

41] Chen

42] Chen

43] Chen

44] Chen

45] Chen

46] Chen

47] Chen

48] Chen

49] Chen

50] Chen

16–19] Chen

15] Chen

16] Chen

17] Chen

18] Chen

19] Chen

20] Chen

21] Chen

22] Chen

23] Chen

24] Chen

25] Chen

26] Chen

27] Chen

28] Chen

29] Chen

30] Chen

31] Chen

32] Chen

33] Chen

34] Chen

35] Chen

36] Chen

37] Chen

38] Chen

39] Chen

40] Chen

41] Chen

42] Chen

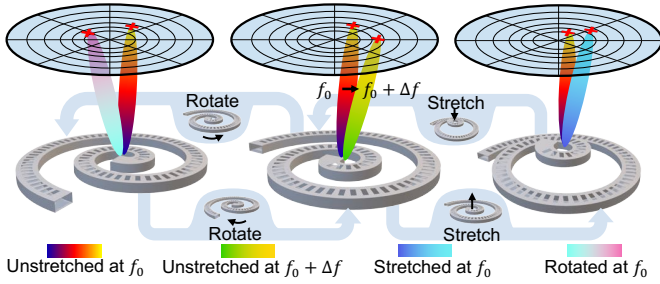


Fig. 3. The schematic diagram of the experimental setup.

$l_a = 22.86 \text{ m}$, $l_b = 10.16 \text{ m}$, $l_t = 1 \text{ m}$, $d_l = 10 \text{ m}$, $d_s = 5 \text{ m}$, $p_d = 10 \text{ m}$, $d_{sc} = 10 \text{ m}$, $e_{sc} = 0$, $t_{sc} = 12 \text{ dB}$.

Fig. 4. A photograph of the experimental setup. The setup includes a Vector Network Analyzer (VNA) KE5071C, a probe, and a device on a table.

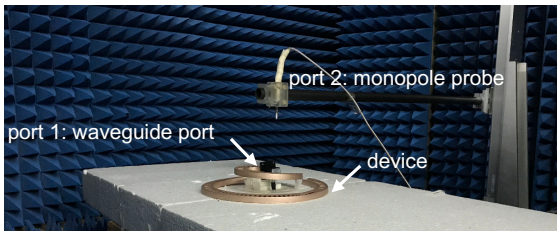


Fig. 4. A photograph of the experimental setup.

Fig. 5. The experimental results showing the rotation and stretching of the ring resonator. The results are presented as polar plots of the scattering parameters S_{11} and S_{21} for different states.

Fig. 5. The experimental results showing the rotation and stretching of the ring resonator. The results are presented as polar plots of the scattering parameters S_{11} and S_{21} for different states. The plots show the phase and magnitude of the scattering parameters as a function of the rotation angle ϕ and the stretching angle θ . The states are labeled as 0000, 0001, and 0010. The rotation angle ϕ ranges from 0° to 315° in increments of 45° . The stretching angle θ ranges from 0° to 180° in increments of 90° . The plots show that the scattering parameters are sensitive to both rotation and stretching, and that the stretching operation can be used to tune the phase and magnitude of the scattering parameters.

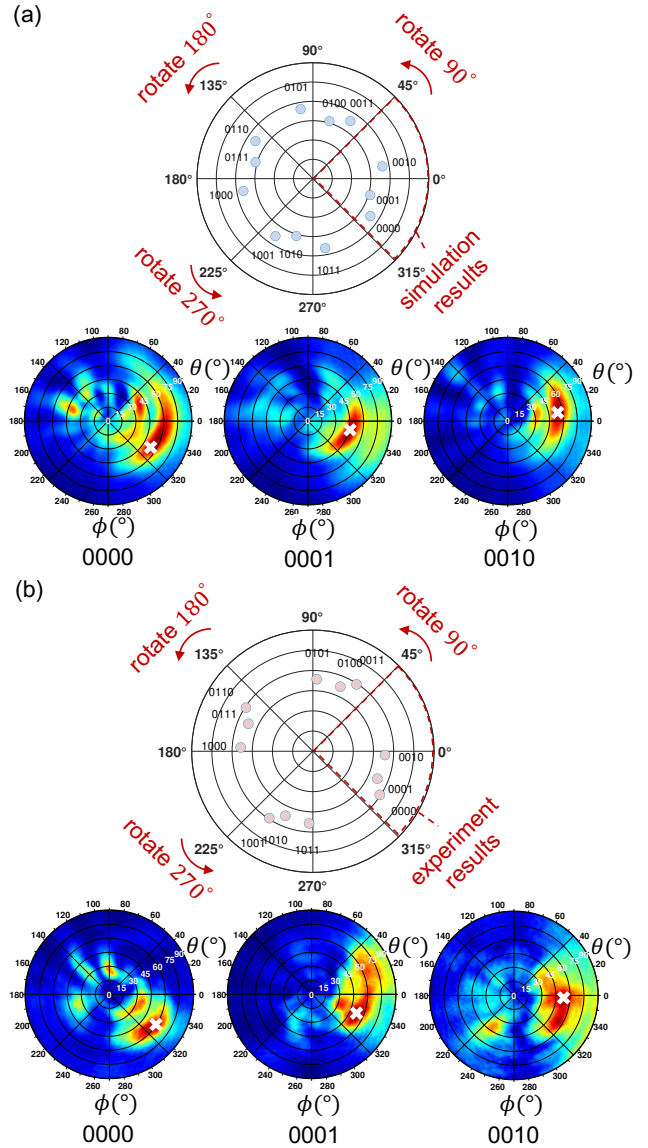


Fig. 5. The experimental results showing the rotation and stretching of the ring resonator.

(a) Simulation results: The simulation results show that the scattering parameters are sensitive to both rotation and stretching. The plots show that the scattering parameters are sensitive to both rotation and stretching, and that the stretching operation can be used to tune the phase and magnitude of the scattering parameters. The states are labeled as 0000, 0001, and 0010. The rotation angle ϕ ranges from 0° to 315° in increments of 45° . The stretching angle θ ranges from 0° to 180° in increments of 90° . The plots show that the scattering parameters are sensitive to both rotation and stretching, and that the stretching operation can be used to tune the phase and magnitude of the scattering parameters.

(b) Experiment results: The experiment results show that the scattering parameters are sensitive to both rotation and stretching. The plots show that the scattering parameters are sensitive to both rotation and stretching, and that the stretching operation can be used to tune the phase and magnitude of the scattering parameters. The states are labeled as 0000, 0001, and 0010. The rotation angle ϕ ranges from 0° to 315° in increments of 45° . The stretching angle θ ranges from 0° to 180° in increments of 90° . The plots show that the scattering parameters are sensitive to both rotation and stretching, and that the stretching operation can be used to tune the phase and magnitude of the scattering parameters.

Table 1. Field

State	* Value	0000	0001	0010	0011	0100	0101	0110	0111	1000	1001	1010	1011
0000	0.057	0.239	0.595	1.180	1.227	1.485	1.611	1.508	1.505	1.100	0.908	0.644	
0001	0.087	0.113	0.458	1.070	1.134	1.412	1.597	1.509	1.539	1.189	1.003	0.766	
0010	0.365	0.192	0.185	0.856	0.954	1.270	1.574	1.519	1.612	1.371	1.198	1.010	

* Value

e The

$$d_{km} = |\hat{\psi}_k \langle \phi_k, \theta_k \rangle - \hat{\psi}_m \langle \phi_m, \theta_m \rangle| \\ = \left[r_c \sin(\phi_k)^2 - 2r_c^2 \cos(\theta_k - \theta_m) \sin(\phi_k) \sin(\phi_m) \right. \\ \left. + r_c \sin(\phi_m)^2 \right]^{\frac{1}{2}}, \quad (6)$$

by $\hat{\psi}_k \langle \phi_k, \theta_k \rangle$ and $\hat{\psi}_m \langle \phi_m, \theta_m \rangle$, in the r_c $1. A$

State 0000, 0001, 0010, 0011, 0100, 0101, 0110, 0111, 1000, 1001, 1010, 1011, 1100, 1101, 1110, 1111. For the state 0000, the value is 0.057.

State 0000, 0001, 0010, 0011, 0100, 0101, 0110, 0111, 1000, 1001, 1010, 1011, 1100, 1101, 1110, 1111. For the state 0001, the value is 0.113. For the state 0010, the value is 0.185.

State 0000, 0001, 0010, 0011, 0100, 0101, 0110, 0111, 1000, 1001, 1010, 1011, 1100, 1101, 1110, 1111. For the state 0000, the value is 0.057. For the state 0001, the value is 0.113. For the state 0010, the value is 0.185.

State 0000, 0001, 0010, 0011, 0100, 0101, 0110, 0111, 1000, 1001, 1010, 1011, 1100, 1101, 1110, 1111. For the state 0000, the value is 0.057. For the state 0001, the value is 0.113. For the state 0010, the value is 0.185.

State 0000, 0001, 0010, 0011, 0100, 0101, 0110, 0111, 1000, 1001, 1010, 1011, 1100, 1101, 1110, 1111. For the state 0000, the value is 0.057. For the state 0001, the value is 0.113. For the state 0010, the value is 0.185.

Funding. National Natural Science Foundation of China (61805097, 61935015, 61825502, 61971174, 61801426, 61801268); National Key Research and Development Program of China (2017YFB1104300); National Science Foundation (20F010018).

Disclosures. The authors have nothing to disclose.

Data Availability. Data are available upon request.

REFERENCES

- L. Peng, L. Duan, K. Wang, F. Gao, L. Zhang, G. Wang, Y. Yang, H. Chen, and S. Zhang, *Nat. Photonics* **13**, 878 (2019).
- D. Schurig, J. J. Mock, B. Justice, S. A. Cummer, J. B. Pendry, A. F. Starr, and D. R. Smith, *Science* **314**, 977 (2006).
- B. Zheng, Y. Yang, Z. Shao, Q. Yan, N.-H. Shen, L. Shen, H. Wang, E. Li, C. M. Soukoulis, and H. Chen, *Res. (Wash. D.C.)* **2019**, 8282641 (2019).
- L. Jing, Z. Wang, X. Lin, B. Zheng, S. Xu, L. Shen, Y. Yang, F. Gao, M. Chen, and H. Chen, *Res. (Wash. D.C.)* **2019**, 3806132 (2019).
- S. Xu, M. Zhang, H. Wen, and J. Wang, *Sci. Rep.* **7**, 1 (2017).
- Z.-Z. Li, L. Wang, H. Fan, Y.-H. Yu, Q.-D. Chen, S. Juodkazis, and H.-B. Sun, *Light. Sci. & Appl.* **9**, 1 (2020).
- W. Chen, T. Yang, L. Dong, A. Elmasry, J. Song, N. Deng, A. Elmarakbi, T. Liu, H. B. Lv, and Y. Q. Fu, *Nanotechnol. Precis. Eng.* **3**, 189 (2020).
- G. Song, C. Zhang, Q. Cheng, Y. Jing, C. Qiu, and T. Cui, *Opt. Express* **26**, 22916 (2018).
- F.-Y. Dong, S. Xu, W. Guo, N.-R. Jiang, D.-D. Han, X.-Y. He, L. Zhang, Z.-J. Wang, J. Feng, W. Su, and H.-B. Sun, *Nano Energy* **77**, 105095 (2020).
- T. Lv, G. Dong, C. Qin, J. Qu, B. Lv, W. Li, Z. Zhu, Y. Li, C. Guan, and J. Shi, *Opt. Express* **29**, 5437 (2021).
- Z. Zhou, Y. Li, H. Li, W. Sun, I. Liberal, and N. Engheta, *Nat. Commun.* **10**, 1 (2019).
- S. Xu, H. Xu, H. Gao, Y. Jiang, F. Yu, J. D. Joannopoulos, M. Soljačić, H. Chen, H. Sun, and B. Zhang, *Proc. Natl. Acad. Sci. U. S. A.* **112**, 7635 (2015).
- J. Sun, M. I. Shalae, and N. M. Litchinitser, *Nat. Commun.* **6**, 1 (2015).
- J. Sun and N. M. Litchinitser, *ACS nano* **12**, 542 (2018).
- S. Sun, Q. He, S. Xiao, Q. Xu, X. Li, and L. Zhou, *Nat. Mater.* **11**, 426 (2012).
- N. Yu and F. Capasso, *Nat. Mater.* **13**, 139 (2014).
- X. Ni, Z. J. Wong, M. Mrejen, Y. Wang, and X. Zhang, *Science* **349**, 1310 (2015).
- C. Qian, B. Zheng, Y. Shen, L. Jing, E. Li, L. Shen, and H. Chen, *Nat. Photonics* **14**, 383 (2020).
- S. Xu, F.-Y. Dong, W.-R. Guo, D.-D. Han, C. Qian, F. Gao, W.-M. Su, H. Chen, and H.-B. Sun, *Sci. advances* **6**, eabb3755 (2020).
- T. J. Cui, M. Q. Qi, X. Wan, J. Zhao, and Q. Cheng, *Light. Sci. Appl.* **3**, e218 (2014).
- Q. Ma and T. J. Cui, *PhotonX* **1**, 1 (2020).
- N.-S. Wu, S. Xu, Z. Wang, and H.-B. Sun, "Reconfigurable slotted antenna inspired by multidimensional modulation," in *2020 IEEE MTT-S International Microwave Workshop Series on Advanced Materials and Processes for RF and THz Applications (IMWS-AMP)*, (2020), pp. 1–3.
- S. Xi, H. Chen, T. Jiang, L. Ran, J. Huangfu, B.-I. Wu, J. A. Kong, and M. Chen, *Phys. Rev. Lett.* **103**, 194801 (2009).
- J. A. Kong, *Electromagnetic wave theory* (EMW Publishing, 2008).
- H. Jiang, K. Xu, Q. Zhang, Y. Yang, D. K. Karmakar, S. Chen, P. Zhao, G. Wang, and L. Peng, *IEEE Trans. Antennas Propag.* **69**, 2987 (2021).
- J. G. Proakis and M. Salehi, *Digital communications*, vol. 4 (McGraw-hill New York, 2001).
- Z. Li, M.-H. Kim, C. Wang, Z. Han, S. Shrestha, A. C. Overvig, M. Lu,

20, 27, 28]

- A. Stein, A. M. Agarwal, M. Lončar, and N. Yu, *Nat. Nanotechnol.* **12**, 675 (2017).
28. R. Zhao, L. Huang, and Y. Wang, *Photonix* **1**, 1 (2020).